Faceting during the Transformation of Amorphous to Crystalline Ice

Michael Mehlhorn and Karina Morgenstern*

Institut für Festkörperphysik, Leibniz Universität Hannover, Appelstrasse 2, D-30167 Hannover, Germany

(Received 29 August 2007; published 12 December 2007)

We study the thermally activated transition from amorphous to crystalline ice (D_2O) on Cu(111) with high-resolution scanning tunneling microscopy. Annealing of amorphous solid water up to the desorption temperature of 149 K results subsequently in monomer decorated double bilayers with different superstructure, a faceted surface, pyramidal islands, and nanocrystallites of distinct height at different coverages. Though all structures are truncations from crystalline water ice, for none of them is the ice bilayer found to be the terminating surface.

DOI: 10.1103/PhysRevLett.99.246101 PACS numbers: 68.43.Hn, 61.46.Df, 68.37.Ef, 68.65.−k

Few physical processes are as ubiquitous or feature more prominently in our daily lives than the nucleation of water into ice. The rich physics and chemistry that arise from the complex interactions between adsorbed water molecules and single crystalline metal surfaces has been investigated for several decades of intense research [1] as a prototype system for understanding water-solid interfaces. Despite this intense research, our knowledge of the structure of adsorbed water remains surprisingly limited, with a number of fundamental questions still to be resolved before general models can be developed for the structure of water at metal surfaces. Even the simplest form of ice on hexagonal surfaces, the so-called bilayer, remains much debated between experiment [2] and theory [3]. Since the interaction of water with surfaces is important to fields as diverse as rain drop nucleation in atmospheric chemistry, fuel cells in electrochemistry, interstellar clouds in astrophysics, and membranes in biophysics, there is an imperative to better understand these processes and to reveal the variety of possible structures developing upon interaction of water with surfaces.

The behavior of water in condensed phases is dominated by intermolecular hydrogen bonds. On metal surfaces, the hydrogen bond energy is comparable to the water-metal interaction [1]. In particular on hexagonal metal surfaces, water is thought to form an extended, hydrogen-bonded network known as ''bilayer ice,'' similar to the (0001) plane found in bulk ice I*h* [1]. This structure contains hexagonal rings, with three water molecules in each ring bound via the lone-pair orbitals of the oxygen to the surface and another three water molecules above them completing the hydrogen-bonded ''bilayer'' structure. Within the hexagonal rings alternating molecules are raised or lowered by 48 pm relative to the central plane to give the proper tetrahedral bonding angles. In dependence of their stacking several bilayers may form the hexagonal I*h* ice or the metastable cubic I*c* ice. By STM, it is not possible to determine the stacking and we will thus refer to both almost isoenergetic crystals [4] in the following.

High-resolution scanning probe studies of the structure of supported water structures provide the only means for obtaining a rigorous molecular-scale description of heterogeneous ice nucleation, because of the variety of possible structures that can be invoked to explain data acquired by indirect means and the variety of isoenergetic structures found in theoretical calculations. However, very few real-space observations of extended ice structures exist [5–7] and high-resolution images of three-dimensional crystalline ice are still awaited for. The difficulty in imaging water is threefold. First, it is easily disturbed by the scanning process due to its large dipole moment and the low energy of a single hydrogen bond [8]. Furthermore, vibrations are easily excited from inelastically tunneling electrons starting from approximately 200 mV [9]. These vibrations might trigger molecule reorientation. Finally, the insulating character of ice layers makes their real height considerably higher than the amount the tip is retracted above the ice layers. This puts a severe limitation on multilayer structure imaging.

In this Letter, we follow the transformation of amorphous solid water (ASW) to crystalline structures of ice between the onset of crystallization (130 K) and of desorption (149 K) on Cu(111), a surface where the lattice mismatch between the basal plane of hexagonal ice I*h* ($a_{\mathrm{ice}} = 0.452$ nm) [or I*c*(111)] and the next nearest neighbor distance of Cu (0.442 nm) is only 2%. At different annealing temperatures surprisingly diverse structures are observed. These can all be explained by hydrogen bonding within the ice network; however, no bilayer termination is observed at any annealing temperature between the crystallization and the desorption temperature. Instead (2×1) superstructures and I*h*{1101} or I*c*{221} are common motifs at different annealing temperatures. This observation shows that more complex ice structures should be invoked, both in theoretical calculations and when interpreting experimental data.

The experiments were performed with a custom-built low temperature STM [10], which facilitates imaging at 0.5 pA. This is important for ice structures because of the large difference in apparent to real height of up to 1.7 nm. Quoted heights throughout this Letter, unless stated as apparent heights, are real heights as determined by tunnel-

ing at 2.9 V into the conduction band of ice [11]. For imaging, parameters were determined that do not influence crystalline ice structures [12].

The Cu(111) surface is cleaned by cycles of Ne^+ sputtering and annealing. The D_2O is degassed in vacuum through freeze-thaw cycles. The D_2O is brought directly to the surface held at 88 K through a molecular tube doser with a rate of 0.3 BL/min. The sample is then transferred into the STM, where measurements are performed at 5 K. For subsequent annealing (heating rate 2 K/s) the sample is transferred back into the preparation chamber with the aid of a He cooled manipulator (20 K). Desorption of D_2O is monitored with a mass spectrometer. The sample is then held for a predefined time at the annealing temperature: for flashing less than 2 s. After having switched off the heater, the sample temperature decreases rapidly (<10 sec) below 40 K. Temperatures were calibrated by a thermocouple and a temperature diode spot welded to a different sample. They are correct absolutely by ± 3 K and relatively by ± 1 K.

We have shown before that amorphous porous water on Cu(111) collapses into amorphous solid water (ASW) through annealing at 118 K [11]. This ASW is the starting point of our experiment. ASW [Fig. 1(a)] is characterized by an arrangement of the molecules (white protrusion) in the top layer without long range order. At 1.1 BL coverage the ASW is 2 to 3 bilayers high. No qualitative changes to ASW layers are observed below an annealing temperature of 125 K, which is thus metastable up to this temperature. Annealing at 130 K and above leads to a variety of crystalline structures [Fig. 1(b)–1(d)].

Extended annealing at 130 K leads to crystallization into the structure shown in Fig. 1(b). A flash to 130 K reveals that islands connected to step edges are the first to crystallize [Fig. 2(a)] as manifested in the hexagonal arrangement of bright protrusions [Fig. 2(b)]. After 5 min annealing the other islands not connected to any step edge are also crystallized. The average height of these islands is (0.90 ± 0.08) nm, which shows them to have the same height as the ASW ice with 2 to 3 bilayers. The lattice distance within the hexagonal arrangement of the topmost molecules is with (0.88 ± 0.05) nm, however, far too large to correspond to molecules hydrogen bonded to each other. Instead, high-resolution images of this intermediate structure [Fig. 2(c)] reveal a honeycomb network *below* the prominent protrusions as expected for a bilayer structure. The unit cell of this network corresponds with (0.43 ± 0.03) nm to the unit cell of Ih(0001) or Ic(111). Line scans reveal an apparent buckling of $(26 \pm 3)\%$ of the apparent bilayer distance d_{BL} [Fig. 2(d)]. Relating this relative value to the real bilayer distance yields a buckling value of (95 ± 11) pm, in excellent agreement with the buckling expected for a bilayer. The imaged layer is the second bilayer above the Cu(111) surface. Thus, the crystallization of ASW on Cu(111) leads to a two-layer slab of bilayer ice, which here is imaged in real space for the first time. The additional molecules are found on top of the upper molecules in the bilayer as expected for a continuation of the crystalline ice. The high-resolution image also demonstrates that the reorganization of the top most molecules into a hexagonal arrangement is indeed indicative of crystallization and thus hydrogen bond rearrangement within the ice at 130 K.

Three different superlattices are observed after the flash to 130 K [Fig. 2(e)–2(g)]. The additional molecules form to 29% the (2×2) overlayer, with respect to the unit cell of

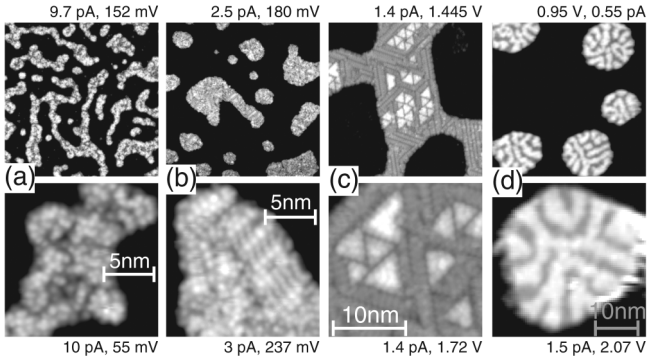

FIG. 1. Annealing of 1.1 BL D_2O on Cu(111). Top panel: overview (85 nm $\times$ 85 nm); bottom panel: details. (a) Annealing at 118 K, (b) annealing at 130 K, (c) annealing at 145 K, (d) flash to 149 K.

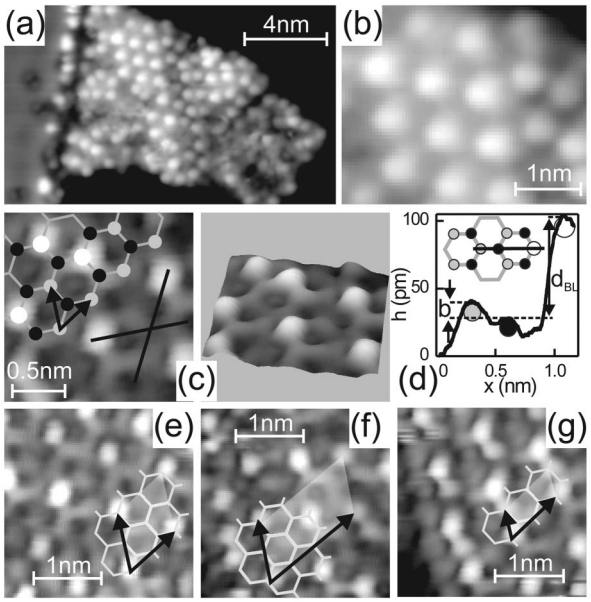

FIG. 2. Beginning of crystallization. (a) Flash to 130 K, (b) magnification of (a), (c) high-resolution image and 3D view of hexagonal bilayer lattice with a functionalized tip. Structure model: molecules in upper part of the bilayer are in gray; in the lower part they are in black. Larger white balls indicate additional monomers hydrogen bonded to upper molecule; bilayer unit cell is indicated by arrows; (d) apparent height of average of the two line scans indicated in (c) with corresponding ball model for determination of the height difference b within the bilayer (see text). (e) (2×2) superstructure on top of bilayer as indicated. (f) $c(2 \times 4)$ superstructure. (g) (2×1) superstructure. (a), (b) 4.8 pA, 167 mV; (c)–(g) 0.11 V, 2.1 pA.

the underlying bilayer, already observed in (b) and to 6% a $c(2 \times 4)$ overlayer, both with a density of 1/8 of a bilayer. The third of the preferred stable termination is to 35% with a density of 1/4 a (2×1) structure, corresponding to well-separated rows of molecules. Within a row the molecules are not directly connected to each other but hydrogen bonded to each second molecule in the underlying bilayer. We point out that on none of the far more than a thousand islands that we imaged after such a flash did we find a hexagonal ice surface without additional molecules. For all superstructures the distance between the molecules is maximized counterintuitive to the often invoked stability of hydrogen-bonded networks. This is first evidence that the bilayer termination is not as energetically favorable as often assumed.

We now return to the structure shown in Fig. 1(b), which is shown in more detail in Fig. 3(a). This structure is stable also for longer annealing times and any annealing at temperatures below 145 K. The structure is characterized by ridges (stripes) that are situated on two complete crystalline bilayers and are oriented along the $\langle 112 \rangle$ direction of the Cu(111) surface. From high-resolution images as shown in Fig. 3(a) the facets of the ridges is determined as I$h\{1101\}$ or I$c\{221\}$. The total height of this structure is 3.5 BL consisting of two complete bilayers, one partial bilayer, and an additional row of molecules with a distance of $2a_{\mathrm{ice}}$.

The complete structure of the ice islands at this annealing temperature consists of parallel ridges in three equivalent domains [cf. Fig. 1(c)]. The width of the ridges varies between 1.3 and 2.6 nm and they are up to 1.5 nm apart. The space between them is filled by a regular arrangement of single molecules, once more in (2×1) superstructure [Fig. 3(a), top left]. Such a local (2×1) arrangement of the molecules is found also in the lowermost row of the facet [Fig. 3(a)].

Annealing the faceted islands to 145 K, i.e., just below the desorption temperature, leads to formation of triangular pyramids that replace the ridges on top of the two bilayers with increasing annealing time [Fig. 1(c)]. These pyramids are oriented in the same direction as the ridges, i.e., along $\langle 112 \rangle$ with respect to Cu(111). The pyramids have one of three distinct sizes with a base length of (2.7 ± 0.2), (4.3 ± 0.3), and (6.0 ± 0.3) nm, corresponding to 6, 10, and 14 ice lattice constants. The structural model is derived from high-resolution images [Fig. 3(b)]. The total height of the pyramids is 4 to 5 bilayers above the surface lattice, consisting of 2 complete bilayers and then up to three successively smaller triangular cuts out of the bilayer. The pyramids are thus not full pyramids, but truncated on the top. The top exhibits a I$h(0001)$ or I$c(111)$ face, but again we never find such a surface without additional molecules, and these once more oriented in one of the superstructures as found upon the first crystallization, most often (2×1). The sides of the pyramids exhibit the same facet as the ridges.

The rearrangement of the former single molecules on top of the bilayer structure into ridges and pyramids is only possible if the molecules diffuse on the underlying ice layer repeatedly forming and breaking hydrogen bonds and if they are promoted into higher layers. Though there is no additional kinetics needed to transform these ridges into a closed bilayer structure, this is not observed. Thus, the completed bilayer is not the favored terminating surfaces of supported ice islands for sizes between 10 and 25 000 nm^2. Instead, faceting of the ice surface is energetically preferred.

This faceting persists up to thermal desorption spectroscopy (TDS)-measurable desorption as shown for flashing at the desorption temperature of 149 K. This annealing leads to a massive rearrangement of the islands to ice crystallites [Fig. 1(d)]. The beginning of such a rearrangement is demonstrated in Fig. 4(a). The front side of the island consists still of two complete bilayers covered with pyramids, while the back side has transformed into a much higher structure. After complete transformation 8 BL, i.e.,

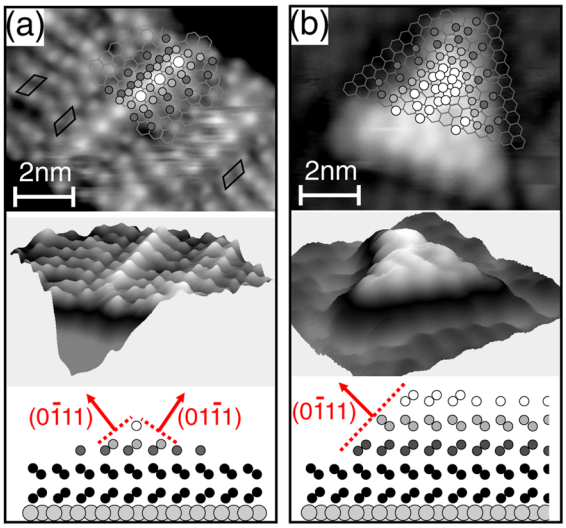

FIG. 3 (color online). Details of crystalline structures: (a) striped structures, 0.11 V, 4.4 pA; (b) pyramidal structure, 1.7 V, 1.4 pA. Top: top view with superimposed model deduced from an extended line scan analysis; each ball corresponds to one molecule. (2×1) is indicated. Middle: 3D view in direction of model shown in a side view in bottom panel for the case of Ih.

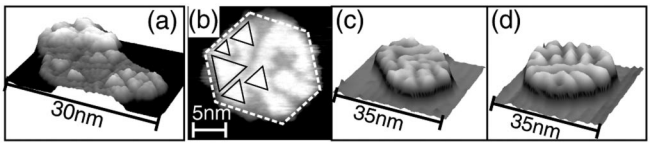

FIG. 4. Ice nanocrystallites upon annealing at desorption temperature: (a) 1.1 BL, flash to 149 K, 1.77 V, 1.4 pA. (b) 1.1 BL, annealing at 149 K for 5 min, 1.64 V, 0.8 pA; contrast variation is consistent with pyramids of indicated size on top of 5 bilayers; straight lines along $\langle 112 \rangle$ of Cu(111). (c) 1.4 BL, flash to 149 K, 2.07 V, 1.5 pA. (d) 2.1 BL, flash to 155 K, 0.95 V, 0.5 pA; same scaling as (c).

>2.5 nm, high crystallites with hexagonal shape are found [Fig. 4(b)].

The top of the nanocrystallites is also not flat as would be expected for bilayer ice, but shows contrast variations of 3 to 4 bilayers in height reminiscent of the ensembles of pyramids discussed above, here, however, situated on top of 5 closed bilayers. The shapes are also consistent with pyramids of the three distinct sizes [Fig. 4(b)].

No qualitative differences in the terminating layers are found when adsorbing 1.4 and 2.1 BL and repeating the annealing experiment with or without intermediate steps. In particular, the height of the nanocrystallites forming through annealing at the desorption temperature is independent from coverage [Fig. 4(c) and 4(d)], i.e., 5 complete bilayers plus 3 incomplete ones.

In conclusion, we give a very detailed account of structures between the onset of crystallization and desorption of water on Cu(111) as an example for a hydrophobic surface. We find no indication of a terminating bilayer at any annealing temperature. Instead, a (2×1) superstructure with a $1/4$ of a BL density and Ih{1101} or Ic{221} are frequently found terminating motifs. Many observations of crystalline ice on metal surfaces, however, were previously interpreted in the sense of the bilayer.

Empirical calculations [13] as well as recent *ab initio* calculations [14] suggested that the adsorption of a single monomer on a bilayer is energetically favorable because undercoordinated water tends to enhance existing hydrogen bonds [15,16]. It remains a theoretical challenge to determine whether this tendency is also responsible for the physical origin of the structures found here.

We believe that our results are quite general and could hold for a variety of other surfaces. For instance, crystallization of amorphous ice layers on hydrophobic Au(111) and on hydrophilic Ru(001) was found to be equivalent in TDS [17]. In addition, we have recently shown that the same type of small ice clusters consisting of six to nine molecules are stable not only on hydrophobic metal surfaces with different lattice constants, but also on some hydrophilic ones [15]. Finally, different studies interpreted their results as the formation of well-separated three-dimensional ice clusters on top of the wetting layer on several hydrophilic surfaces [18]. Furthermore, a weak evidence for a (2×2) superstructure was found on top of a 250 bilayer thick water film on Pt(111) investigated by He scattering [19]. Because the ridges and pyramids observed here are situated on two or even five bilayers with the lattice constants of the free bilayer, we believe that structures not terminated by bilayers should be considered also on top of the wetting layer on hydrophilic surfaces or even when ice grows on ice. Many models invoked so far to interpret experimental data on ice structures might thus have been too simple.

We acknowledge financial support from the Deutsche Forschungsgemeinschaft. We thank A. Michaelides, LCN, for critical reading of the manuscript.

*morgenstern@fkp.uni-hannover.de

[1] M. A. Henderson, Surf. Sci. Rep. **46**, 1 (2002).
[2] H. Ogasawara, B. Brena, D. Nordlund, M. Nyberg, A. Pelmenschikov, L. G. M. Pettersson, and A. Nilsson, Phys. Rev. Lett. **89**, 276102 (2002); K. Andersson, A. Nikitin, L. G. M. Pettersson, A. Nilsson, and H. Ogasawara, Phys. Rev. Lett. **93**, 196101 (2004); J. Weissenrieder, A. Mikkelsen, J. N. Andersen, P. J. Feibelman, and G. Held, Phys. Rev. Lett. **93**, 196102 (2004); S. Haq, C. Clay, G. R. Darling, G. Zimbitas, and A. Hodgson, Phys. Rev. B **73**, 115414 (2006).
[3] P. J. Feibelman, Science **295**, 99 (2002); S. Meng, L. F. Xu, E. G. Wang, and S. Gao, Phys. Rev. Lett. **89**, 176104 (2002); A. Michaelides, A. Alavi, and D. A. King, Phys. Rev. B **69**, 113404 (2004); S. Meng, E. G. Wang, Ch. Frischkorn, M. Wolf, and S. Gao, Chem. Phys. Lett. **402**, 384 (2005); G. Materzanini, G. F. Tantardini, P. J. D. Lindan, and P. Saalfrank, Phys. Rev. B **71**, 155414 (2005).
[4] Y. Paul Handa, D. D. Klug, and E. Whalley, J. Chem. Phys. **84**, 7009 (1986); S. Casassa, M. Calatayud, K. Doll, C. Minot, and C. Pisani, Chem. Phys. Lett. **409**, 110 (2005).
[5] J. Cerda, A. Michaelides, M.-L. Bocquet, P. J. Feibelman, T. Mitsui, M. Rose, E. Fomin, and M. Salmeron, Phys. Rev. Lett. **93**, 116101 (2004); T. Yamada, S. Tamamori, H. Okuyama, and T. Aruga, Phys. Rev. Lett. **96**, 036105 (2006).
[6] M. Morgenstern, Th. Michely, and G. Comsa, Phys. Rev. Lett. **77**, 703 (1996).
[7] T. Mitsui, M. K. Rose, E. Fomin, D. F. Ogletree, and M. Salmeron, Science **297**, 1850 (2002).
[8] K. Morgenstern and J. Nieminen, J. Chem. Phys. **120**, 10 786 (2004).
[9] K. Morgenstern, H. Gawronski, M. Mehlhorn, and K. H. Rieder, J. Mod. Optic. **51**, 2813 (2004).
[10] M. Mehlhorn, H. Gawronski, L. Nedelmann, A. Grujic, and K. Morgenstern, Rev. Sci. Instrum. **78**, 033905 (2007).
[11] J. Stähler, M. Mehlhorn, U. Bovensiepen, M. Meyer, D. O. Kusmierek, K. Morgenstern, and M. Wolf, Phys. Rev. Lett. **98**, 206105 (2007).
[12] In extended voltage and current series we determined these to be <2.5 V for crystalline ice with <10 pA for the water islands and <1.5 pA for the nanocrystals.
[13] E. R. Batista and H. Jonsson, Comput. Mater. Sci. **20**, 325 (2001).
[14] C. Thierfelder, A. Hermann, P. Schwerdtfeger, and W. G. Schmidt, Phys. Rev. B **74**, 045422 (2006).
[15] A. Michaelides and K. Morgenstern, Nature Mater. **6**, 597 (2007).
[16] P. Wernet *et al.*, Science **304**, 995 (2004).
[17] R. Scott Smith, C. Huang, E. K. L. Wong, and B. D. Kay, Surf. Sci. **367**, L13 (1996).
[18] G. A. Kimmel, N. G. Petrik, Z. Dohnalek, and B. D. Kay, Phys. Rev. Lett. **95**, 166102 (2005); T. Kondo, H. S. Kato, M. Bonn, and M. Kawai, J. Chem. Phys. **126**, 181103 (2007); S. Haq and A. Hodgson, J. Phys. Chem. C **111**, 5946 (2007).
[19] A. Glebov, A. P. Graham, A. Menzel, J. P. Toennies, and P. Senet, J. Chem. Phys. **112**, 11 011 (2000).